QUANTITATIVE MAPPING OF HYDRATION IN LUNAR PYROCLASTIC DEPOSITS: INSIGHTS INTO WATER FROM THE LUNAR INTERIOR. S. Li[1] and R. E. Milliken[1], [1]Department of Geological Sciences, Brown University, RI, 02912, shuai_li@brown.edu

Introduction: Pyroclastic deposits on the Moon represent early lunar volcanic processes [1], and models of explosive volcanism indicate that the range of pyroclastic deposits is proportional to volatile content [2]. Therefore, the distribution of lunar pyroclastic deposits and their estimated water content can provide indirect information on the distribution of volatiles in magma source regions [3]. In return, knowledge of interior volatile content, any spatial heterogeneity, and how it may vary with depth or through time can improve our understanding of lunar magma ocean models and provide constraints for the loss or retention of volatiles during the Moon formation event. Moreover, these pyroclastic deposits are potential sources for water and other in situ resources for future exploration [4].

Here we discuss the mapping of 'water' (H_2O/OH) content of lunar pyroclastic deposits using Moon Mineralogy Mapper (M^3) visible-near infrared surface reflectance spectra. Our previous quantitative mapping results of global hydration with M^3 data showed that surface hydration is dominantly controlled by latitude and local surface temperature [5]. There was almost no detectable hydration between 30° N and 30° S latitude on the lunar surface, which suggests any hydration bonds (i.e., OH) formed superficially by solar wind implantation are likely broken by high surface temperatures during local lunar daytime. This indicates hydration formed by solar wind implantation is not stable over long periods at these latitudes and will likely not accumulate to significant degrees for typical surface materials.

In contrast, pyroclastic deposits in these latitudes exhibit increased hydration signals even at local noon [5]. In this study we focus on pyroclastic deposits between 30° N and 30° S and, to avoid ambiguity in identifying small pyroclastic deposits (e.g., <1000 km^2), analyze those classified as 'large' deposits by [6]. We analyze the relationship between water content and other characteristics including mineralogical, chemical, spectral, topographic, and morphological characteristics for eleven large pyroclastic deposits in this study region.

Methods: The Effective Single Particle Absorption Thickness (ESPAT) parameter at 2.9μm is linearly correlated with absolute water content for a wide variety of minerals [7]. The lunar surface hydration map (ESPAT) adopted from *Li and Milliken* [2013] (Figure 1) is used as a proxy for hydration. Our recent lab analyses have shown that the slope of the linear ESPAT - wt.% H_2O trend is ~2 for synthetic volcanic glasses, and we are currently carrying out experiments for determining the slope of this trend for anorthosite and other relevant lunar compositions.

Average ESPAT and total areas for the eleven pyroclastic deposits (marked with yellow circles in Figure 1) were calculated. Figure 1 shows that the eleven pyroclastic deposits are highly hydrated and have distinct boundaries with the surrounding regions. We used the Region of Interest (ROI) tool in the ENVI software to calculate the average ESPATs and total areas for these deposits (Figure 2).

M^3 reflectance spectra for these pyroclastics were extracted and analyzed to compare their possible mineralogical and chemical compositions. Topography data were extracted from the Lunar Orbiter Laser Altimeter (LOLA) data and resized to the same spatial resolution as our hydration (ESPAT) map (1km/pixel).

Results and Discussion: Pyroclastic deposits at Aristarchus, Montes Harbinger, Sulpicius Gallus, Rima Bode, and Humorum (five of the eleven) exhibit extensively high abundances of hydration (e.g., >1500ppm on average), whereas Moscoviense, Taurus Littrow, Montes Carpatus, and Vaporum (four of the eleven) show moderately high abundance of hydration (~800 ppm on average). Nectaris has lower hydration (~500ppm) and Aestuum shows no detectable hydration.

The relationship between areal coverage of pyroclastics and average ESPAT for ten large pyroclastic deposits (not including Aestuum) is plotted in Figure 2. The linear trend shown in Figure 2, to a first order, is consistent with volcanic explosion models that suggest pyroclastic range is directly proportional to volatile content [2]. This is also consistent with the majority of observed hydration being representative of endogenous volatiles and heterogeneity in lunar magma volatile contents. However, past models have primarily considered CO as the dominant volatile, thus it may be worth to re-examining those models to consider the role of H_2O in the amounts predicted here.

No detectable hydration at Aestuum might indicate a relatively volatile-poor magma source region. Alternatively, previous studies with telescopic data suggest Aestuum is less homogenous than other pyroclastic deposits and might be contaminated by surrounding highlands [8], thus its true water content may simply be obscured by dilution from non-pyroclastic materials. Aestuum may be a pyroclastic flow deposit (low volatile, low explosivity), whereas the five highly hydrated pyroclastics may be pyroclastic fall deposits (high volatiles, highly explosive). Reflectance spectra at pyroclastic fall deposits are expected to be brighter than those at

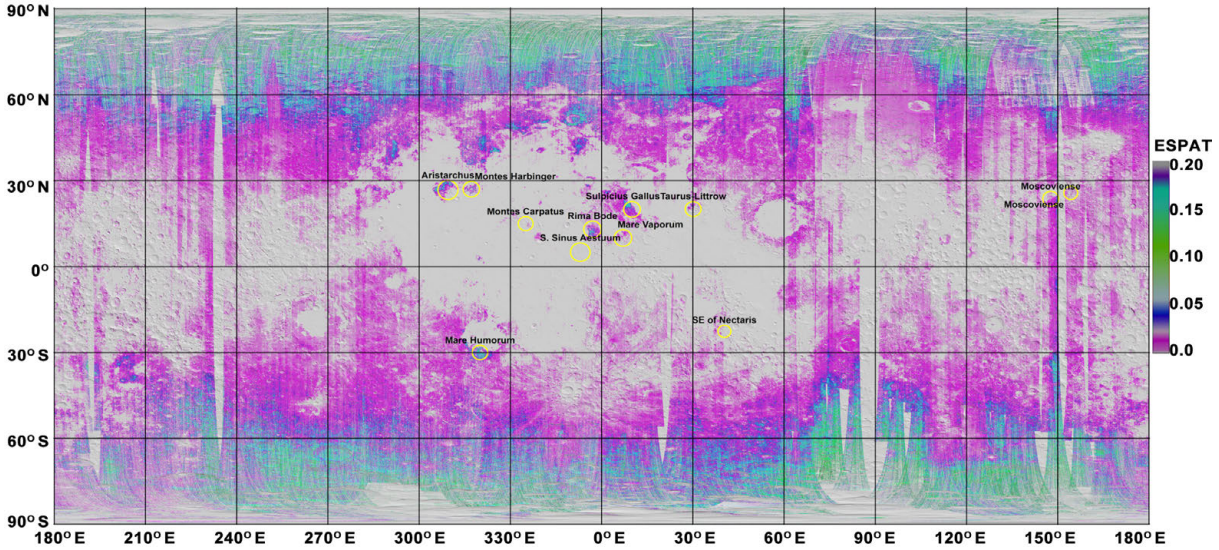

Figure 1. Quantitative mapping of lunar surface hydration (ESPAT) and large pyroclastic deposits (yellow circles) between 30°N and 30°S; wt.% water can be estimated by multiplying the ESPAT value by 2 for pyroclastic deposits.

pyroclastic flow deposits because of finer grained material on upper portions of the deposits, which is consistent with M^3 reflectance spectra for these pyroclastic deposits.

Current results indicate that not all lunar pyroclastic deposits exhibit hydration signatures, and this is true even for smaller deposits not discussed here. In addition, there is a wide range in apparent water content between various deposits. A number of factors may explain these variations (space weathering effects on spectral properties, covering or dilution by volatile-poor components, loss of volatiles in glasses over time). However, these variations may reflect real differences in the volatile contents of magma source regions or different degrees of magma degassing during ascent and eruption. In addition, preliminary results for Sulpicius Gallus indicate that the highest water contents are not associated with clear morphological features such as vents, though not all vents may be apparent in orbital images. Future work will focus on detailed morphologic analyses of thes e deposits as they relate to water distribution and assessment of how water content of various deposits may inform us of specific ascent and eruption conditions through geologic time

Conclusions: Large pyroclastic deposits between 30° N and 30° S exhibit increased hydration that is inconsistent with solar wind implantation. Unlike nearby regions, these zones are highly hydrated even under the hottest surface conditions (at local noon) and continue to exhibit up to ~1000 ppm H_2O. Areas of pyroclastic deposits are linearly correlated with estimated water contents which to a first order is consistent with volcanic explosion models. Aestuum exhibits no detectable hydration and might be a low-volatile content pyroclastic flow deposit, whereas highly hydrated pyroclastics may be fall deposits. Current results suggest hydration and thus volatile content of magma source regions for lunar pyroclastics are heterogeneous. This information can help to constrain lunar magma ocean models, lunar volcanism styles through time, and volatile retention as a result of the Moon formation event.

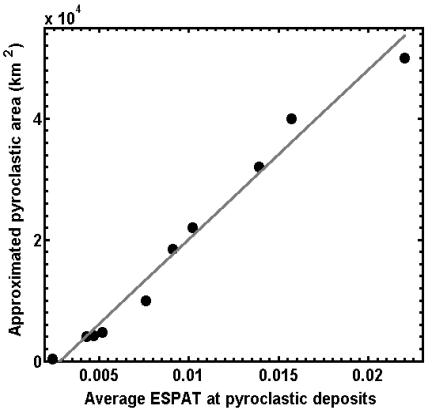

Figure 2. Relationship between pyroclastic deposit areas and average ESPAT values (linear proxy for water content).

References: [1] Head, J. W. (1976). *Rev Geophys* 14. [2] Fagents, S. A. and Wilson, L. (1993). *Geophys J Int* 113. [3] Saal, A. E. *et al.* (2008). *Nature* 454. [4] Hawke, B. R. *et al.* (1990) *P Lunar Planet Sci C*. [5] Li, S. and Milliken, R. (2013) *Lunar Planet Sci C*. [6] Gaddis, L. R. *et al.* (2003). *Icarus* 161. [7] Milliken, R. E. and Mustard, J. F. (2005). *J Geophys Res-Planet* 110. [8] Pinori, S. and Bellucci, G. (2001). *Planet Space Sci* 49.